

Available online at [ScienceDirect](http://ScienceDirect)

# Nuclear Engineering and Technology

journal homepage: [www.elsevier.com/locate/net](http://www.elsevier.com/locate/net)

## Original Article

# Numerical Comparison of Thermalhydraulic Aspects of Supercritical Carbon Dioxide and Subcritical Water-Based Natural Circulation Loop

Milan Krishna Singha Sarkar and Dipankar Narayan Basu\*

Department of Mechanical Engineering, Indian Institute of Technology Guwahati, Guwahati, Assam – 781039, India

### ARTICLE INFO

#### Article history:

Received 16 February 2016

Received in revised form

6 September 2016

Accepted 7 September 2016

Available online xxx

#### Keywords:

Heat Transfer Deterioration

Natural Circulation

Single Phase

Supercritical

Thermalhydraulics

### ABSTRACT

Application of the supercritical condition in reactor core cooling needs to be properly justified based on the extreme level of parameters involved. Therefore, a numerical study is presented to compare the thermalhydraulic performance of supercritical and single-phase natural circulation loops under low-to-intermediate power levels. Carbon dioxide and water are selected as respective working fluids, operating under an identical set of conditions. Accordingly, a three-dimensional computational model was developed, and solved with an appropriate turbulence model and equations of state. Large asymmetry in velocity and temperature profiles was observed in a single cross section due to local buoyancy effect, which is more prominent for supercritical fluids. Mass flow rate in a supercritical loop increases with power until a maximum is reached, which subsequently corresponds to a rapid deterioration in heat transfer coefficient. That can be identified as the limit of operation for such loops to avoid a high temperature, and therefore, the use of a supercritical loop is suggested only until the appearance of such maxima. Flow-induced heat transfer deterioration can be delayed by increasing system pressure or lowering sink temperature. Bulk temperature level throughout the loop with water as working fluid is higher than supercritical carbon dioxide. This is until the heat transfer deterioration, and hence the use of a single-phase loop is prescribed beyond that limit.

Copyright © 2016, Published by Elsevier Korea LLC on behalf of Korean Nuclear Society. This is an open access article under the CC BY-NC-ND license (<http://creativecommons.org/licenses/by-nc-nd/4.0/>).

## 1. Introduction

The basic concept of a natural circulation loop (NCL) is to have energy transmission from a heat source to a heat sink, connected by adiabatic arms through a closed circuit, without bringing them in direct contact and also without involving any

rotating machinery. The density difference between the fluids flowing through two vertical sections of the loop develops buoyancy, which acts as the driving potential. It is mandatory to locate the sink at a higher elevation than the source, to take advantage of the favorable density gradient. Geometrical simplicity and enhanced passive safety of NCLs have attracted

\* Corresponding author.

E-mail addresses: [dipankar.n.basu@gmail.com](mailto:dipankar.n.basu@gmail.com), [dnbasu@iitg.ernet.in](mailto:dnbasu@iitg.ernet.in) (D.N. Basu).

<http://dx.doi.org/10.1016/j.net.2016.09.007>

1738-5733/Copyright © 2016, Published by Elsevier Korea LLC on behalf of Korean Nuclear Society. This is an open access article under the CC BY-NC-ND license (<http://creativecommons.org/licenses/by-nc-nd/4.0/>).

diverse technical applications including solar water heaters, refrigeration systems, thermosyphon reboilers, and cooling of rotating machineries as well as transformers, electronic chips, and nuclear reactor core. Inherent reliability of such loops, due to the absence of moving elements, makes them particularly suitable for large-scale nuclear systems, and hence adoption of both single- and two-phase versions of NCLs can be observed in industries. A supercritical natural circulation loop (SCNCL) is a relatively newer concept and is expected to lead nuclear reactors toward higher thermal efficiency in comparison with the other versions, owing to its higher range of operating pressure and temperature. The system is also more compact due to the elimination of bulky components such as steam generator, dryer, and steam separator. Therefore, the concept of a supercritical water reactor has evolved as one of the most promising technologies under the generation-IV reactors. Water remains the most common working fluid in applications involving temperature above 0°C, whereas various brines are employed for low-temperature cases. However, the nontoxic and nonexplosive nature of supercritical CO<sub>2</sub> (sCO<sub>2</sub>), coupled with its excellent heat transfer performance, has projected sCO<sub>2</sub> as the next-generation coolant. It is safe, chemically stable, economically viable, and environment friendly [1], which has encouraged several research groups to explore sCO<sub>2</sub>-based SCNCLs.

While most of the experimental and theoretical investigations focused on high-power operation of SCNCLs, a few of the recent efforts were directed toward medium-to-low power applications. Chen et al [2,3] experimented on a CO<sub>2</sub>-based SCNCL in the power range of 65–189 W, to study the steady-state thermalhydraulics and stability behavior at different pressures. Heat transfer coefficient on the heater side was found to decrease with an increase in bulk temperature. Consequently, loop thermalhydraulics was found to depend on several parameters inclusive of the temperature differential between the heater and cooler, operating pressure, channel diameter, relative orientation of the heater and cooler, and inclination angle [4]. Heat transfer efficiency of the loop was reported to decrease with increasing operating temperature and is higher for larger-diameter loops, as was numerically identified by Chen et al [5]. In fact, with a continuous increase in input power, SCNCLs can exhibit heat transfer deterioration (HTD), characterized by a rapid decline in mass flow rate and heat transfer coefficient, accompanied by a sharp increase in maximum fluid temperature, as was demonstrated by Sarkar and Basu [6]. Appearance of HTD was found to depend on both system pressure and sink temperature. Sharma et al [7–9] conducted an experimental, as well as numerical, study to analyze the effect of heater and cooler orientation on steady-state behavior. Mass flow rate was found to increase until the heater inlet temperature reached a pseudocritical value. Successful use of commercial software for the simulation of an SCNCL was demonstrated by Yadav et al [10,11]. Asymmetry in velocity and temperature profiles was observed, which was attributed to the three-dimensional (3-D) variation in fluid parameters owing to the presence of bends and local buoyancy. Effects of unsteady heat input and inclination angle (0–90°) were numerically studied by Chen et al. [12,13] over a wide range of input heat flux. Influence of inclination on the average Nusselt number was found to be of

lesser significance at lower heat fluxes, but very important for higher powers. A periodic change in the pressure field was observed due to the typical distribution of temperature-sensitive thermophysical properties of sCO<sub>2</sub>, which led to repetitive flow reversals [5,14]. More comprehensive discussion on the steady-state thermalhydraulics of an SCNCL can be found in the study by Sarkar et al [15].

A systematic literature survey, therefore, suggests that the thermalhydraulic aspects of an SCNCL have received considerable attention over the last decade, with particular emphasis on high-power systems for nuclear core cooling. However, with the advent of portable reactors [16], loops operating at low-to-intermediate power levels definitely have an enormous scope, along with possible applications in solar heaters and refrigerators. It is common to employ single-phase NCLs for such systems, despite the saturation temperature constraint and low flow limitation. As a single-phase loop is a well-explored device, its thermalhydraulic and stability responses are generally well documented [17], which is its prime advantage over SCNCLs, along with the moderate levels of working parameters. Therefore, implementation of supercritical loops for low-power situations over its single-phase counterpart needs to be justified, and the present work attempts precisely the same. A comparative thermalhydraulic analysis was performed by developing a 3-D computational model of a rectangular NCL. Water was selected as the working fluid for the single-phase loop and CO<sub>2</sub> for the supercritical one. Operating conditions were selected so that the respective states can be maintained for both the fluids under an identical set of working parameters. Effects of system pressure, heater power, and sink temperature were examined to explore the relative merits of either loops and make a final recommendation accordingly.

## 2. Computational model and numerical procedure

### 2.1. Physical geometry

A rectangular loop of uniform diameter was chosen for the present analysis, as shown in Fig. 1. The diameter ( $D$ ), height ( $H$ ), and width ( $L$ ) of the loop are 8 mm, 800 mm, and 600 mm, respectively. The heater and cooler were placed in the middle of the opposite horizontal arms, with both having identical length ( $L_h = L_c$ ) of 400 mm. Stainless steel was selected as the wall material with 1 mm thickness. Accordingly, a 3-D numerical model was developed using ANSYS-Fluent 15 (ANSYS Inc., Canonsburg, PA, USA). The focus of the present study being thermalhydraulic analysis at low-to-intermediate powers, selected power levels are limited to 700 W.

### 2.2. Conservation equations

Steady-state versions of 3-D mass, momentum, and energy conservation equations were solved using ANSYS-Fluent 15 (ANSYS Inc.), along with the equations of state for the concerned fluids. The operating range of Reynolds number being invariably in the turbulence regime, a renormalized group

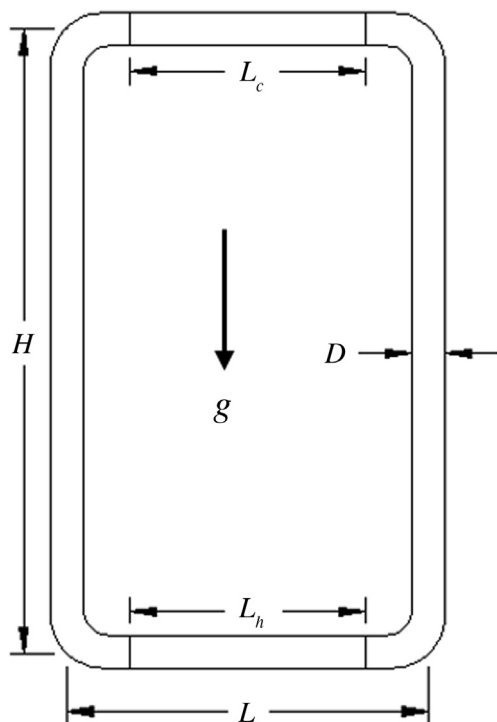


Fig. 1 – Schematic diagram of the rectangular loop.

$k - \epsilon$  model was employed by the following relevant literature [5,10,18]. The complete set of governing equations is summarized below.

Conservation of mass:

$$\frac{\partial}{\partial x_j} (\rho u_j) = 0 \quad (1)$$

Conservation of momentum:

$$\frac{\partial}{\partial x_j} (\rho u_j u_i) = -\frac{\partial p}{\partial x_i} + \frac{\partial \tau_{ji}}{\partial x_j} + \rho g_i \quad (2)$$

Here, the shear stress ( $\tau_{ji}$ ) is defined as follows:

$$\tau_{ji} = \mu_{\text{eff}} \left( \frac{\partial u_i}{\partial x_j} + \frac{\partial u_j}{\partial x_i} - \frac{2}{3} \delta_{ij} \frac{\partial u_k}{\partial x_k} \right) \quad \mu_{\text{eff}} = \mu + \mu_t = \mu + C_\mu \rho \frac{k^2}{\epsilon} \quad (3)$$

Conservation of energy:

$$\frac{\partial}{\partial x_j} (\rho u_j h) = \frac{\partial}{\partial x_j} \left( \lambda_{\text{eff}} \frac{\partial T}{\partial x_j} + u_j \tau_{ji} \right) + S_E \quad (4)$$

Here,  $\lambda_{\text{eff}}$  is the modified thermal conductivity and  $S_E$  represents the external energy source term. It is positive in the heater section, negative in the cooler, and zero elsewhere.

### 2.3. Numerical scheme of solution

The selected set of conservation equations was solved using ANSYS-Fluent 15 (ANSYS Inc.) following the implicit finite volume method. Pressure terms were discretized using PRESTO, whereas second-order discretization was used for all other terms. Pressure Implicit with Splitting of Operator (PISO) algorithm was selected for resolving the pressure–velocity coupling. Axial conduction in the tube wall was taken into

consideration and no-slip boundary condition was imposed at the fluid–wall interface, while assuming standard wall functions to facilitate the near-wall treatment.

Properties of any supercritical fluid vary drastically around the pseudocritical point. The variation is moderate for the single-phase medium, but can be significant in deciding the interaction between buoyancy and friction. Therefore, an accurate estimation of thermodynamic and transport properties plays a vital role in any NCL simulation. National Institute of Standards and Technology (NIST) standard reference database (version 9.1; NIST, Gaithersburg, MD, USA) is built within each ANSYS-Fluent 15 (ANSYS Inc.) session to estimate the value of all thermophysical properties as functions of local pressure and temperature.

A system of structured grids was developed over the entire computational domain at the ANSYS-Fluent 15 (ANSYS Inc.) workbench. In order to capture larger near-wall gradients of the flow variables, nonuniform grids were applied, with finer meshes close to the wall (Fig. 2). Finer axial meshes were employed in the heat-exchanging sections, as well as at the corners, with larger meshes in the vertical arms. A grid sensitivity analysis was performed to ensure the correctness of the output. Simulations were performed with three different grid structures and the corresponding observations were summarized (Table 1) for the sCO<sub>2</sub> loop with an operating pressure of 8.5 MPa. Associated heating power and sink temperature are 330 W and 298 K, respectively. As a 3-D approach is followed with total property variation, fluid velocity, and temperature at any point vary along all the three coordinate directions. For comparison purpose, average quantities were used, and this referred to the averaged value across the midplanes of all horizontal and vertical arms. With a 23% increase in the number of cells from Model 2 to Model 1, changes in average values are limited to 0.5% over the entire range of parameters considered, which can be considered to be acceptable, and hence Model 2 is adopted for further

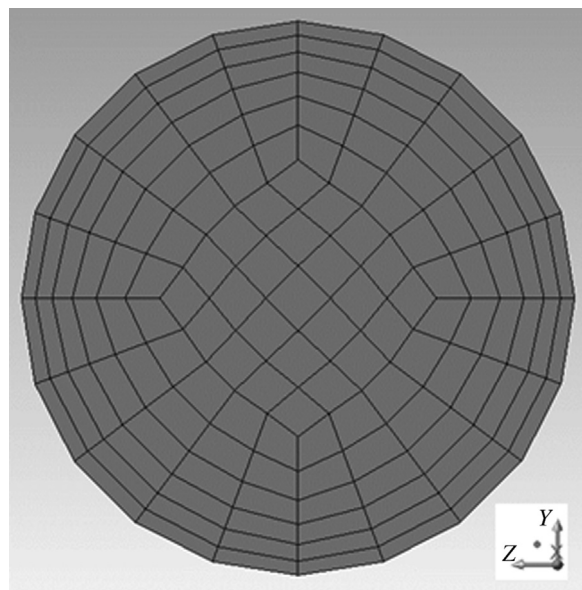


Fig. 2 – Cross-sectional view of mesh distribution at the source center.

**Table 1 – Details of employed grid system.**

	Model 1	Model 2	Model 3
Number of nodes	141,516	115,088	89,836
Number of cells	119,952	97,020	75,264
Average velocity (m/sec)	0.7339	0.7304	0.7214
Average temperature (K)	335.199	335.211	335.424

analysis. The corresponding mesh geometry also has decent values of average skewness (0.14) and orthogonal quality (0.976). The magnitude of wall  $y^+$  is an indicator of turbulence in the flow field. The selected mesh system provides  $y^+ = 41.45$  for an sCO<sub>2</sub>-based loop with 8.5 MPa pressure and 300 W heater power, which ensures accurate selection of a turbulence model. A cross-sectional view of the adopted grid system at the source center is shown in Fig. 2.

### 3. Results and Discussion

The key motivation of the present computational investigation is the thermalhydraulic comparison of single-phase and supercritical NCLs with low-to-intermediate power input, commonly found in solar heaters, electronic cooling devices, and heat pipes [19–21], and can be suitable for portable reactors. Therefore, heater power was selected within the range of 10–700 W. Three different pressure levels were selected for analysis, namely, 7.5 MPa, 8.5 MPa, and 9.5 MPa, with all the values being above the critical pressure of CO<sub>2</sub> (~7.38 MPa) and well below the same for water (~22.06 MPa). This ensures the supercritical nature for CO<sub>2</sub> and allows water to remain as a single-phase liquid depending on the imposed temperature level. Variation in the sink temperature was reported to affect the flow field and heat transfer aspects of an SCNCL [5,6,11], and hence the effect of the same was also explored meticulously. It is important to note that system pressure refers to the absolute pressure at some reference location of the loop. Bulk pressure varies along the loop length and is generally scaled relative to that value. The magnitude of such variation over the entire loop was found to be less than 0.11 kPa, which is negligible in comparison to system pressure, and hence the discussion on loop thermalhydraulics can conveniently be presented in terms of system pressure.

#### 3.1. Validation with experimental data

To substantiate the correctness of the computational results, it is essential to correlate these with comparable experimental results. Fig. 3 presents the validation plot for the sCO<sub>2</sub>-based loop using the relation proposed by Swapnalee et al [22]. Among the four correlations proposed by them, the one for the horizontal-heater–horizontal-cooler configuration was compared with the present simulation data for 8.5 MPa system pressure, 298 K sink temperature, and input power range of 10–500 W. The steady-state solution at any particular heater power was converted to Reynolds and Grashof numbers, and they were employed to characterize the system. An excellent agreement can be observed, which endorses the use of the computational model for subsequent appraisal.

#### 3.2. Effect of local buoyancy development

Owing to the strongly coupled nature of momentum and thermal diffusion in an NCL, it is likely to have significant variation of fluid temperature and local velocity across any cross section, which, in turn, is dependent on the level of operating parameters and imposed boundary conditions. Fig. 4 presents the velocity and temperature contours at the midplanes of the sCO<sub>2</sub>-based loop and water-based single-phase NCL, respectively, under identical conditions. Both the loops exhibit significant asymmetry in respective profiles, with substantially larger irregularity in the SCNCL. At the heater section, temperature of fluid layers next to the wall is much higher than that of the bulk fluid. Similarly, fluid temperature near the wall of the cooler is reasonably close to the sink temperature and is considerably lower than that of the fluid near the centerline. Therefore, fluid density varies over any cross section, with the lighter fluid close to the heater wall surrounding much heavier fluid, thereby developing a local buoyancy effect. While the fluid in contact with the lower portion of the wall attempts to move upward due to buoyancy, the lighter fluid around the upper portion of the wall remains virtually immobile. This acts somewhat like an obstruction to the flow field, providing an added acceleration at the lower portion of the channel. This explains the higher velocity of this portion for the heater section. Lower velocity around the top wall also allows higher residence time to the fluid, increasing the temperature level there. The reverse is true for the cooler, with the heavier and cooler fluid close to the bottom surface and a lower velocity level. Cross-sectional variation in fluid viscosity may also have a role to play, as the warmer fluid will experience lesser viscous resistance during its upward motion along the heater wall, leading to a further enhancement in local velocity magnitude. However, the relative variation in viscosity with temperature is much lesser compared with density, particularly around the pseudocritical point, and hence the local buoyancy is expected to be the governing factor in determining cross-sectional profiles.

Density variation for the single-phase liquid is much lesser, and hence the water loop presents more regularized profiles (Fig. 5), with a moderate inclination toward the lower wall in the heater and upper wall in the cooler. Properties of water and sCO<sub>2</sub> are compared in Fig. 6. Thermal conductivity of single-phase water is nearly five times of that for sCO<sub>2</sub> and increases with temperature until the appearance of a peak. By contrast, thermal conductivity for sCO<sub>2</sub> reduces sharply around the pseudocritical point. This ensures much better temperature distribution within water and better heat transfer behavior. The asymmetry is much less pronounced in the vertical adiabatic arms, as all the fluid particles in a cross section experiences identical influence of gravity and hence local buoyancy is relatively weaker.

#### 3.3. Mass flow rate deterioration

The extent of such asymmetry and temperature variation over a cross-section, however, is strongly reliant on the imposed boundary conditions. A small change in the fluid temperature level can lead to substantial alteration in the properties of supercritical fluid, which can consequently result in



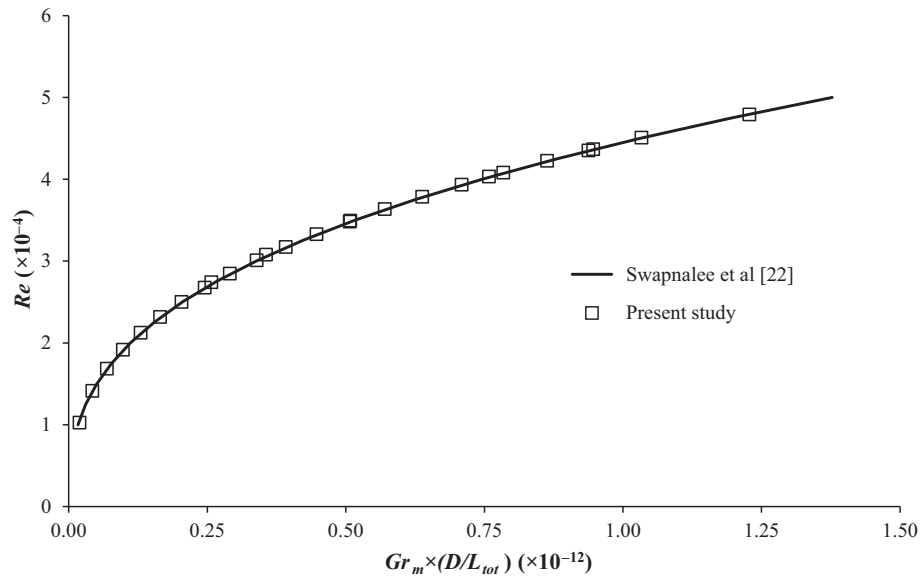


Fig. 3 – Comparison of present model prediction with existing literature for a supercritical CO<sub>2</sub> loop.

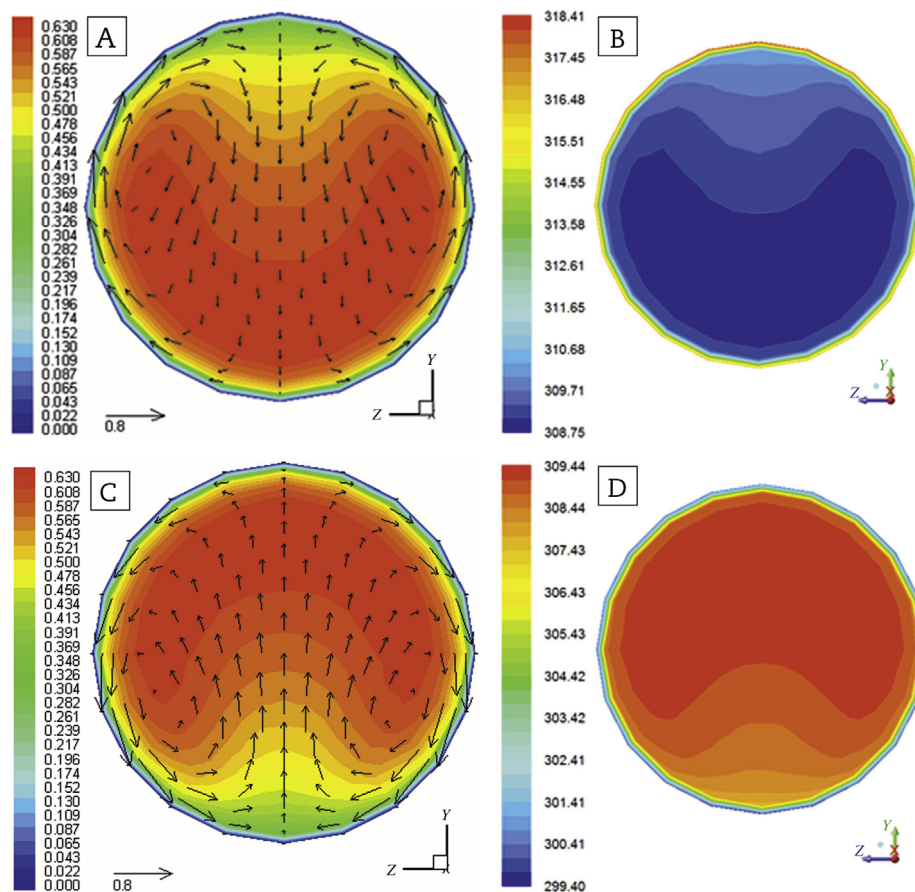
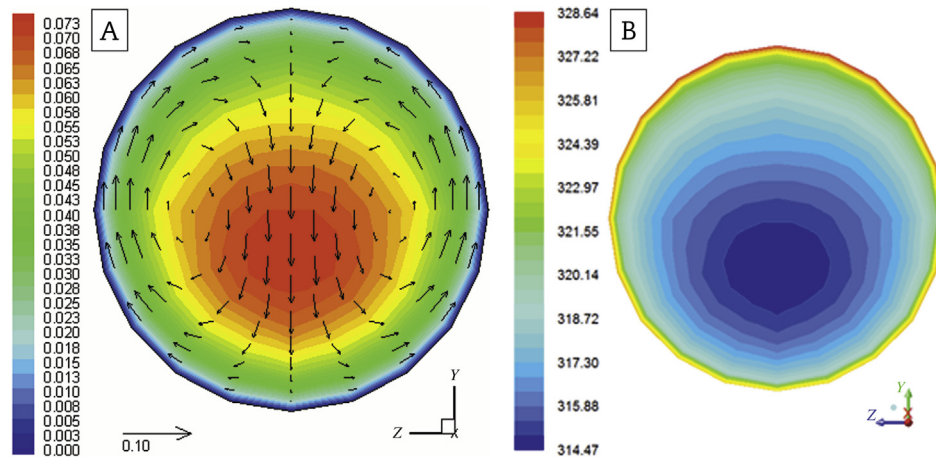


Fig. 4 – Velocity and temperature contours. (A and C) Velocity and (B and D) temperature contours at (A and B) source and (C and D) sink centers of sCO<sub>2</sub>-based loop for 8.5 MPa pressure with 298 K sink temperature and 320 W input power. sCO<sub>2</sub>, supercritical carbon dioxide.

contrasting loop behavior. The flow field in an NCL is generated by an interplay between buoyancy and frictional forces, with the driving buoyancy being proportional to the effective density difference. When the fluid was allowed to cross the

pseudocritical point inside the heat-exchanging sections, a significant density difference is available due to the gas-like lighter fluid in the riser and liquid-like heavier fluid in the downcomer. Accordingly, buoyancy dominates the frictional



**Fig. 5 – Water loop profiles. (A) Velocity and (B) temperature contours at source center of water-based loop for 8.5 MPa pressure with 298 K sink temperature and 320 W input power.**

forces, and the loop flow rate continually increases with heater power for a specified sink temperature, as can be seen from Fig. 7. Around the pseudocritical point, volumetric expansion coefficient assumes a peak and density drops sharply. Therefore, when the minimum fluid temperature inside the loop crosses the pseudocritical value, there was a rapid decline in the effective buoyancy, despite significant temperature differential across the heater. Frictional forces start controlling the flow beyond such a power level.

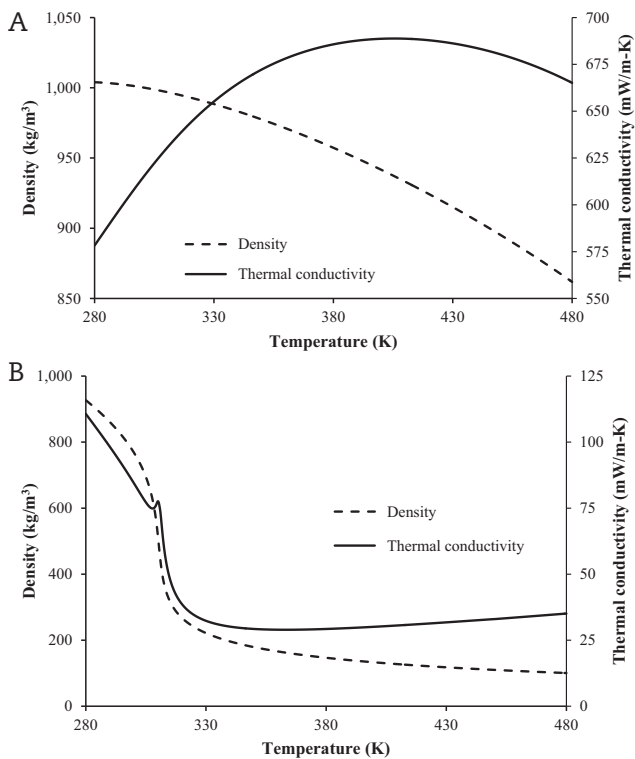


**Fig. 6 – Properties of water and sCO<sub>2</sub>. Variation of density and thermal conductivity of (A) water and (B) CO<sub>2</sub> with temperature for 8.5 MPa pressure.**

Consequently, a rapid decline in mass flow rate can be observed, which continues to decrease at a moderate rate thereafter. Such deterioration in mass flow rate in SCNCLs has also been observed experimentally [7–9] and through a 2-D numerical model [23]. Effect of such a drastic change in mass flow rate on the thermal field can be recognized by comparing the temperature contours at the source center for two different situations (Fig. 8). With only 10 W rise in the input power, CO<sub>2</sub> experiences about 63 K temperature variation in a single cross section, compared with just about 10 K in the other case. Axial profiles of bulk temperature over the entire loop length for sCO<sub>2</sub> and water for two different conditions were compared, as shown in Fig. 9. In case of 320 W input power, a large mass flow rate results in moderate temperature variation for sCO<sub>2</sub> over the loop and about 24 K lower value of maximum fluid temperature compared with water. However, with only 10 W increase in power, heater inlet temperature can clearly be seen to be above the pseudocritical value, resulting in substantial temperature variation across the loop. The maximum value of bulk temperature for sCO<sub>2</sub>

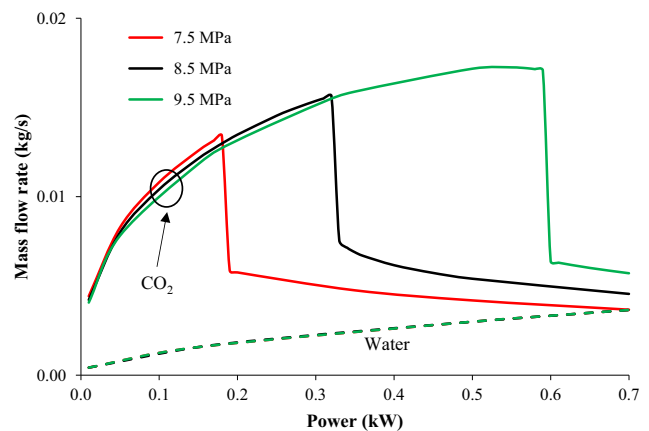


**Fig. 7 – Variation of mass flow rate with power and system pressure for 298 K sink temperature.**

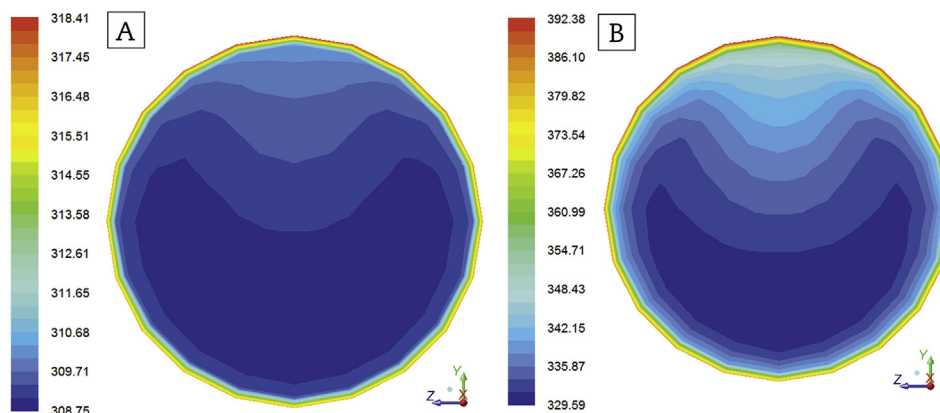


**Fig. 8 – Source-center temperature contours of sCO<sub>2</sub>-based loop for 8.5 MPa pressure and 298 K sink temperature and different input powers. (A) 320 W. (B) 330 W. sCO<sub>2</sub>, supercritical carbon dioxide.**

can be about 12 K higher than that for water under identical operating conditions.

Variation in bulk fluid temperature for a heater inlet and outlet with power is presented in Fig. 10. It is clearly evident that the maximum fluid temperature, expected to appear around the heater outlet, remains around the pseudocritical value until a certain power level, which steeply increases with the rise in sink temperature. Beyond that limit, however, both temperatures increase drastically. A large mass flow rate ensures small temperature differential across the heater until the abovementioned power limit. For higher powers, the temperature rise, experienced by the fluid across the heater, increases sharply, forcing the bulk temperature profiles to veer away from each other. The conclusion can also be drawn here about the role of the sink temperature. A cooler sink reduces the overall temperature level of the loop fluid and hence allows it to stay below the pseudocritical limit until higher power values, thereby facilitating operation with a large flow rate and low bulk temperature in the heater outlet. As can be seen from Fig. 10, the outlet temperature can be maintained at a low value until about 320 W with  $T_c = 298$  K, while power drops to around 100 W with only 10 K rise in  $T_c$ . This hints toward a possible mechanism of reducing the sink

temperature at higher powers, in order to sustain high flow rates and avoid any drastic rise in temperatures.

Pseudocritical temperature increases with pressure, which allows the supercritical fluid to avail much higher power levels, before it attains the maxima in mass flow rate at elevated pressures (Fig. 7). For 9.5 MPa system pressure, the sCO<sub>2</sub>-based loop realizes the maxima around 0.59 kW, compared with about 0.31 kW for 8.5 MPa pressure, despite only about 11% rise in the magnitude of that maximum value. Therefore, it is suggested to operate the SCNCL at higher pressure levels, as this will allow the system to have a larger mass flow rate over a wider span of power, thereby keeping the fluid temperature levels in control. Density of single-phase water follows more regular variation with temperature, and hence a monotonic increase in mass flow rate can be observed with heater power. The mass flow rate value for sCO<sub>2</sub> is significantly higher than that of water at lower powers. Accordingly, the temperature level associated with water loop is higher than that for sCO<sub>2</sub>, which can be substantiated comparing the temperature contours presented earlier. Owing to the incompressible nature, pressure hardly has any effect on the performance of the single-phase system, apart from redefining the saturation temperature constraint.

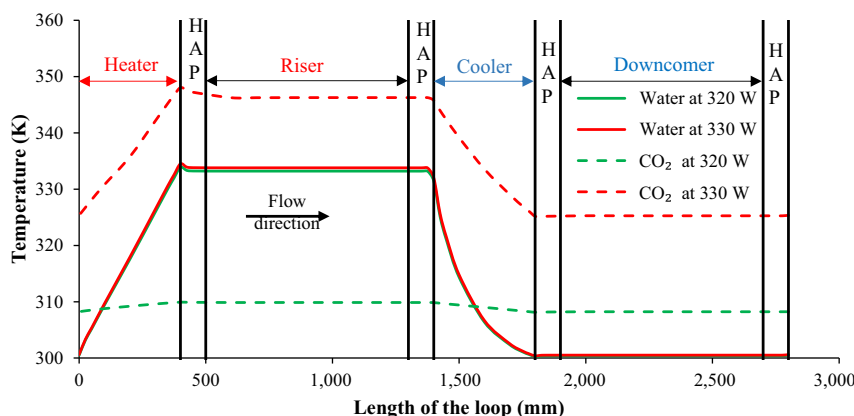


**Fig. 9 – Axial profile of fluid bulk temperature for 8.5 MPa pressure and 298 K sink temperature and different input powers. HAP, horizontal adiabatic portion.**

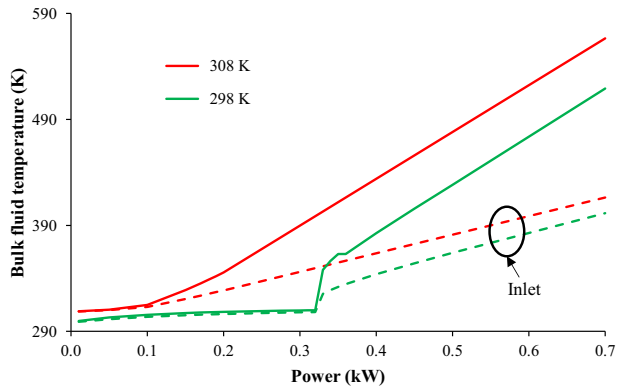


**Fig 10 – Variation of bulk fluid temperatures at heater inlet and outlet with input power for different sink temperatures and 8.5 MPa pressure.**

### 3.4. Appearance of HTD

Fig. 11 shows the variation in sink-side average heat transfer coefficient with heater power for different pressure levels of  $s\text{CO}_2$  and also water. Heat transfer coefficient at any location is a function of local Reynolds number ( $Re$ ) and Prandtl number ( $Pr$ ). Changes in  $Re$  with power level is substantial due to the changes in mass flow rate, while  $Pr$  decreases at a moderate rate beyond the pseudocritical point. Therefore, the heat transfer coefficient closely follows the mass flow rate profile. For an  $s\text{CO}_2$ -based SCNCL, it rapidly increases with power until the maximum is reached and suffers a drastic fall thereafter for all the pressure levels, with the maxima appearing around the same power level as for the mass flow rate. Hence, this particular power level can be identified as the initiation of HTD in an SCNCL. It also corresponds to a rise in the maximum fluid temperature and so is directly related to the material-related safety concerns. Therefore, the HTD location is an important landmark during any SCNCL operation, and heater power should be regulated to maintain below this limit, in order to have higher mass flow rate and heat transfer coefficient, while maintaining a lower fluid temperature level. It is important to mention here that the term HTD is commonly employed for forced flow channels with wall heating to signify a drastic reduction in heat transfer coefficient and a simultaneous increase in wall temperature, without any significant change in

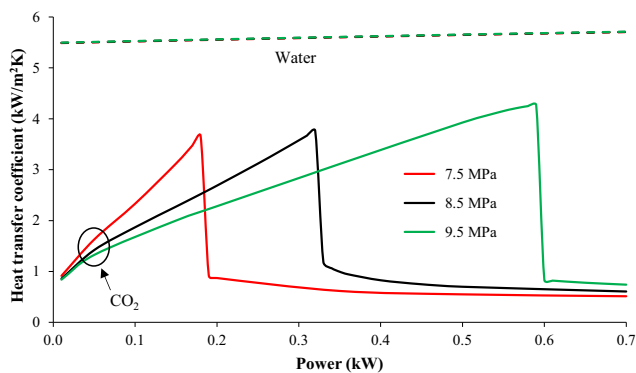


**Fig. 11 – Variation of heat transfer coefficient with power and system pressure for 298 K sink temperature.**

fluid temperature, while the flow rate remains constant. The situation is a bit different for an SCNCL, as the fluid temperature may exhibit a sharp rise due to the reduction in flow rate. The natural circulation version of HTD is, in fact, deterioration in heat transfer coefficient as a consequence of a deterioration in mass flow rate and therefore can also be termed as flow-induced heat transfer deterioration (FiHTD) to differentiate it from forced flow systems.

Heat transfer coefficient predicted for a single-phase water loop was found to be consistently higher than that for an SCNCL. This can be attributed to the higher thermal conductivity of the working fluid (Fig. 6), particularly in the cooler section. Therefore, the single-phase loop was expected to offer more consistent heat transfer performance than the SCNCL. The SCNCL offered a larger mass flow rate and a significantly lower fluid temperature level, thereby projecting itself as a superior option, until the appearance of FiHTD. However, the operator needs to be careful about the FiHTD constraint, and the system must not be allowed to reach the maxima of mass flow rate.

## 4. Conclusion

Computational performance appraisal of a 3-D rectangular NCL is presented here to compare the thermalhydraulic aspects of  $\text{CO}_2$  and water as working media under low-to-intermediate power levels. Operating conditions were selected so as to maintain  $\text{CO}_2$  in a supercritical state and water as a single-phase liquid. Effects of system pressure, sink temperature, and heater power were systematically explored to reach the following conclusions. (1) Significant amount of asymmetry can be observed in both velocity and temperature profiles at any cross section in the horizontal arms due to local buoyancy effects. Extent of such asymmetry is more prominent for  $s\text{CO}_2$ -based loop due to substantial property variation around the pseudocritical point. (2) Increase in power enhances the density differential across the heater, yielding substantial buoyancy force and hence a continuous increase in mass flow rate until a maximum is reached. As the lowest fluid temperature crosses the pseudocritical limit, a sharp decline in mass flow rate can be observed, owing to the weakening of buoyancy. This leads to a drastic deterioration in heat transfer coefficient and hence can be identified as a practicable limit of operation. (3) The power level corresponding to the appearance of FiHTD can be increased by raising pressure and lowering sink temperature. A mechanism can also be devised to maneuver the sink temperature with heater power for delaying the appearance of such deterioration. (4) A single-phase water-based loop presents a monotonic profile of mass flow rate, magnitude of which is well below that of an SCNCL, until the appearance of FiHTD, leading to an elevated temperature level. The heat transfer coefficient for a single-phase water-based NCL is consistently higher than that for an SCNCL, owing to higher thermal conductivity of the working fluid.

Overall, it can be concluded that an  $s\text{CO}_2$ -based SCNCL can be a superior choice, as long as the power level can be limited to FiHTD, owing to the higher flow rate and lower fluid temperature levels. This makes it a decent choice for low-to-



intermediate power levels. For example, with 9.5 MPa system pressure and 298 K sink temperature, a CO<sub>2</sub>-based SCNCL can be employed until about 0.59 kW power, which perfectly suits several industrial applications. The loop under consideration has a dimension of 0.8 m × 0.6 m, which is appropriate for solar heaters and refrigeration devices, and hence the observations from the present study can directly be extrapolated to an experimental prototype. However, if the expected power range of operation goes beyond the FiHTD constraint, single-phase water-based loops are clearly a better option, due to their consistent behavior. High-pressure requirement can be another deterring issue for SCNCLs. In addition, the stability analysis and dynamic performance assessment need to be carried out for an SCNCL before drawing a final conclusion, and this can be viewed as the next step of research.

### Conflict of interest

Present work has no conflict of interest.

### Acknowledgments

Financial support for this study was provided by the Department of Science and Technology (DST), India, under SERB fast track project for young scientists (vide sanction no. SERB/F/5300/2012-13, dated December 19, 2012) is gratefully acknowledged.

### Nomenclature

A	cross-sectional area (m <sup>2</sup> )
C <sub>p</sub>	specific heat (J/kg K)
D	diameter (m)
g	gravitational acceleration (m/s <sup>2</sup> )
Gr <sub>m</sub>	modified Grashof number (= $g\beta D^3 \rho^2 \dot{Q}H / A\mu^3 C_p$ )
h	enthalpy (J/kg)
H	height (m)
k	turbulent kinetic energy (m <sup>2</sup> /s <sup>2</sup> )
L	length (m)
$\dot{m}$	mass flow rate (kg/s)
p	pressure (N/m <sup>2</sup> )
P	wetted perimeter (m)
Pr	Prandtl number (= $\mu C_p / \lambda$ )
$\dot{Q}$	input power (W)
Re	Reynolds number (= $\rho u D / \mu$ )
S <sub>E</sub>	source of energy (W/m <sup>3</sup> )
T	temperature (K)
u	velocity (m/s)
W	width (m)
x	space coordinate

### Greek symbols

$\beta$	volumetric expansion coefficient (1/K)
$\delta_{ij}$	Kronecker delta
$\varepsilon$	turbulent dissipation rate (m <sup>2</sup> /s <sup>3</sup> )
$\lambda$	thermal conductivity (W/m K)

$\rho$	density (kg/m <sup>3</sup> )
$\mu$	dynamic viscosity (kg/m s)
$\tau$	shear stress (N/m <sup>2</sup> )

### Subscripts and superscripts

c	cooler
eff	effective
h	heater
pc	pseudocritical
t	turbulent
tot	total

### REFERENCES

- [1] G. Lorentzen, J. Pettersen, A new, efficient and environmentally benign system for car air-conditioning, *Int. J. Refrig* 16 (1993) 4–12.
- [2] L. Chen, B.L. Deng, X.R. Zhang, Experimental investigation of CO<sub>2</sub> thermosyphon flow and heat transfer in the supercritical region, *Int. J. Heat Mass Transfer* 64 (2013) 202–211.
- [3] L. Chen, B.L. Deng, X.R. Zhang, Experimental study of trans-critical and supercritical CO<sub>2</sub> natural circulation flow in a closed loop, *Appl. Therm. Eng* 59 (2013) 1–13.
- [4] Y. Cao, X.R. Zhang, Flow and heat transfer characteristics of supercritical CO<sub>2</sub> in a natural circulation loop, *Int. J. Therm. Sci.* 58 (2012) 52–60.
- [5] L. Chen, B.L. Deng, B. Jiang, X.R. Zhang, Thermal and hydrodynamic characteristics of supercritical CO<sub>2</sub> natural circulation in closed loops, *Nucl. Eng. Des* 257 (2013) 21–30.
- [6] M.K.S. Sarkar, D.N. Basu, Working regime identification for natural circulation loops by comparative thermalhydraulic analyses with three fluids under identical operating conditions, *Nucl. Eng. Des* 293 (2015) 187–195.
- [7] M. Sharma, D.S. Pilkhwal, P.K. Vijayan, D. Saha, R.K. Sinha, Steady-state behavior of natural circulation loops operating with supercritical fluids for open and closed loop boundary conditions, *Heat Transfer Eng* 33 (2012) 809–820.
- [8] M. Sharma, P.K. Vijayan, D.S. Pilkhwal, Y. Asako, Steady state and stability characteristics of natural circulation loops operating with carbon dioxide at supercritical pressures for open and closed loop boundary conditions, *Nucl. Eng. Des* 265 (2013) 737–754.
- [9] M. Sharma, P.K. Vijayan, D.S. Pilkhwal, Y. Asako, Natural convective flow and heat transfer studies for supercritical water in a rectangular circulation loop, *Nucl. Eng. Des* 273 (2014) 304–320.
- [10] A.K. Yadav, M.R. Gopal, S. Bhattacharyya, CFD analysis of a CO<sub>2</sub> based natural circulation loop with end heat exchangers, *Appl. Therm. Eng* 36 (2012) 288–295.
- [11] A.K. Yadav, M.R. Gopal, S. Bhattacharyya, CO<sub>2</sub> based natural circulation loops: new correlations for friction and heat transfer, *Int. J. Heat Mass Transfer* 55 (2012) 4621–4630.
- [12] L. Chen, X.R. Zhang, S. Cao, H. Bai, Study of trans-critical CO<sub>2</sub> natural convective flow with unsteady heat input and its implications on system control, *Int. J. Heat Mass Transfer* 55 (2012) 7119–7132.
- [13] L. Chen, X.R. Zhang, B.L. Deng, B. Jiang, Effects of inclination angle and operation parameters on supercritical CO<sub>2</sub> natural circulation loop, *Nucl. Eng. Des* 265 (2013) 895–908.
- [14] X.R. Zhang, L. Chen, H. Yamaguchi, Natural convective flow and heat transfer of supercritical CO<sub>2</sub> in a rectangular circulation loop, *Int. J. Heat Mass Transfer* 53 (2010) 4112–4122.
- [15] M.K.S. Sarkar, A.K. Tilak, D.N. Basu, A state-of-the-art review of recent advances in supercritical natural circulation loops

- for nuclear applications., *Ann. Nucl. Energy* 73 (2014) 250–263.
- [16] E.F. Clark, *Camp Century: Evolution of Concept and History of Design, Construction and Performance*, Technical Report, United States Army Materiel Command Cold Regions Research and Engineering Laboratory, 1965.
- [17] D.E. Ruiz, A. Cammi, L. Luzzi, Dynamic stability of natural circulation loops for single phase fluids with internal heat generation, *Chem. Eng. Sci.* 126 (2015) 573–583.
- [18] L. Chen, X.R. Zhang, Simulation of heat transfer and system behavior in a supercritical CO<sub>2</sub> based thermosyphon: effect of pipe diameter, *J. Heat Transfer* 133 (2011) 2505–2513.
- [19] P.E. Tuma, H.R. Mortazavi, Indirect thermosyphon for cooling electronic devices, *Electron. Cooling* 12 (2006) 26–32.
- [20] B.Y. Tong, T.N. Wong, K.T. Ooi, Closed-loop pulsating heat pipe, *Appl. Therm. Eng.* 21 (2001) 1845–1862.
- [21] S. Khandekar, M. Groll, An insight into thermos-hydrodynamic coupling in closed loop pulsating heat pipes, *Int. J. Therm. Sci.* 43 (2004) 13–20.
- [22] B.T. Swapnalee, P.K. Vijayan, M. Sharma, D.S. Pilkhwal, Steady state flow and static instability of supercritical natural circulation loops, *Nucl. Eng. Des.* 245 (2012) 99–112.
- [23] V. Archana, A.M. Vaidya, P.K. Vijayan, Numerical modeling of supercritical CO<sub>2</sub> natural circulation loop, *Nucl. Eng. Des.* 293 (2015) 330–345.